FLUORESCENTLY LABELED MAGNETIC MICORBEADS FOR EXPERIMENTAL SINGLE MOLECULAR MECHANICS

By

Maryann Morales

A capstone project submitted for
Graduation with University Honors

May 31, 2020

University Honors
University of California, Riverside

APPROVED

_____
Dr. Valentine Vullev
Department of Bioengineering

_____
Dr. Richard Cardullo, Howard H Hays Jr. Chair, University Honors

Abstract

Fluorescent dyes have served as probes for biological systems for a long time. Despite the huge amount of dyes available, the needs for new fluorescence probes with high emission quantum yields, improved chemical and photostability, acceptable water solubility, and with functional groups that allow for covalent labeling, are currently increasing to meet the demands of all novel modalities of optical microscopy. Naphthalimides are relatively easy to synthesize from inexpensive commercially available materials and have been extensively used for studying charge transfer in organic media. Their pronounced charge-transfer character of the lowest excited state of 6-amino naphthalimides gives them distinct solvatochromatic properties. Polar solvents stabilize the excited state causing bathochromic spectral shifts. However, naphthalimides lack solubility in water, and the use of aqueous media is essential for biological systems. There are immensely limited number of examples of water-soluble naphthalimides, this presents a motivation for the search for derivatives of this dye that can serve as photoprobes. We observe that the addition of a single positive charge, in the form of protonatable amine on an alkyl chain, making the aminonaphthalimide water soluble, without compromising its lipophilicity. This aminonaphthalimide, indeed, demonstrates strong solvatochromism. In addition, we observe that an increase in solvent polarity lowers its emission quantum yield and shortens its excited-state lifetime by orders of magnitude. This property is consistent with the significant change of excited-state geometry resultant from the formation of a TICT state. As the polarity-induced energy of the TICT excited-state is lowered it improves its Franck-Condon overlap with the ground-state significantly increasing the non-radiative deactivation rates. Along with its solubility in water and solvatochromism, the sensitivity of its emission quantum yield to media polarity makes this dye an excellent candidate for probing cellular microenvironment, that we have already tested with Gram-positive and Gram-negative bacteria. In future work, ANI can be used as fluorescent tag on the bead surface providing a means for improving the sensitivity of the imaging tracking that is used for following single-molecule events. These studies will provide means for detection of transition states and for discerning directionality of interactions.

Introduction

The recent renascence in optical imaging has brought revolutionary advances in life sciences by offering improved spatial and temporal resolution (Liu et al., 2018)(Eilers et al., 2018)(Sahl & Moerner, 2013). Some of the most important breakthroughs in the field encompass various fluorescence modalities (Zhao et al., 2018) .These developments place high demands on chemists in the search for fluorophores that not only have pronounced photostability, facile means for conjugations, high emission quantum yields, and molar extinction coefficients, but also feature sensitivities to biologically pertinent characteristics of microenvironments.

Even in the 21st century, infectious diseases remain the leading cause of deaths in low-income communities and countries.(Anderson & Chu, 2007)The current COVID-19 pandemic, along with other recent outbreaks, demonstrates that communicable diseases can have socioeconomic impacts on a global scale.(Smith et al., 2019) Optical microscopy provides a means for expedient *in situ* visualization not only of bacterial cells, but also of viruses, thanks to the recent advances in sub-diffraction-limit microscopy.(Rust et al., 2006)(Li et al., 2013)

Reliable staining of bacterial and viral species is paramount for their optical imaging and detection.(Ettinger & Wittmann, 2014)(Caldwell et al., 1992) The required copious washing for removing the unbound chromophore from the background, along with the implementation of fixation steps that often kill the cells, presents challenges and limitations for the applicability of optical staining. Employing principles of molecular photo physics, such as solvatochromism and emission enhancement, provides a means for differentiating the stained cells from the background signals from the unbound dye.

Fluorescent agents with high specificity, such as immunostains, are indeed incomparable for labeling specific cells and organelles. Pathogens in the samples that are not targeted by such

high-specificity tests, however, remain undetected. In addition to the binary outcomes, i.e., “stain” vs. “does not stain,” monitoring extra characteristics, such as morphology of cells and kinetics of staining, arms low-specificity tests with capabilities for further discernibility between bacterial species.(Thomas et al., 2010)(Upadhyayula et al., 2012)

Employing molecular-rotor dyes, such as thioflavin T (ThT) and cyanines, allowed our group to demonstrate high-contrast fluorescence imaging not only of prokaryotic cells, but also of bacterial endospores while maintaining their vitality. (Xia et al., 2011)(Thomas et al., 2010)(Upadhyayula et al., 2012) This first examples of non-destructive imaging of bacterial endospores with ThT allows for monitoring in real time sporulation of Gram positive bacteria and germination of endospores. (Xia et al., 2011)The fluorescence quantum yields of these molecular-rotor chromophores increase with orders of magnitude when transferred from the low-viscosity aqueous surrounding to the rigid binding microenvironment in the cell walls and the endospore coats.(Xia et al., 2011)(Upadhyayula et al., 2015) That is, the left-over unbound dye (tens and hundreds μM) in the liquid medium surrounding the cells does not fluoresce strongly enough to generate background that interferes with the quality of the images.(Xia et al., 2011) Conversely, the dye taken up by the cells generates a readily detectable fluorescence signal (Xia et al., 2011)(Thomas et al., 2010; Upadhyayula et al., 2012)

In addition to the rigidity, polarity is another key characteristic of the binding microenvironment of biological systems (Gonçalves, 2010). While solvatochromism offers an excellent means for probing the polarity of binding sites, shifting of the spectral maxima is not enough for suppressing the undesired signal from the free unbound photoprobes in the surrounding. Conversely, introducing charge-transfer (CT) character in the excited state can result not only in solvatochromism of the optical spectra, but also in polarity-induced fluorescence

quenching(Majumdar & Basu, 1960). An increase in media polarity lowers the energy levels of excited states with CT character, causing bathochromic spectral shifts.(Heitele et al., 1989) In some cases, however, a further polarity increase brings the CT excited states low enough to the ground states to induce the formation of conical intersections that provide pathways for efficient non-radiative decays via internal conversion mediated by back CT (Domcke & Yarkony, 2012). This feature is perfect for imaging that utilizes lipophilic binding sites. Indeed, the realization of such imaging modalities relies on stains that are practically non-fluorescent in the surrounding aqueous media, while the uptake by cells or tissues turns on their emission.

As intricate components of numerous organic CT systems, aromatic imides are relatively easy to synthesize from readily available materials. The pronounced CT character of the lowest singlet excited state of the derivatives of 4-amino-1,8-naphthalimide (ANI) makes them attractive chromophores that absorb and fluoresce in the visible spectral region and exhibiting pronounced solvatochromism. Naphthalimides, however, have low to negligible solubility in water, which renders them impractical for biological applications (Singha et al., 2015). While adding multiple charges on ANI derivatives can address this issue, it can also decrease the affinity of these chromophores for lipophilic binding sites.(Wahadoszamen et al., 2014)

Herein, we demonstrate that adding a single positive charge to ANI is enough to make it water soluble for biological studies, without compromising its solubility in organic solvents. When in aqueous media, ANI is practically non-fluorescent, exhibiting short excited-state lifetime, τ = 13 ps, and small fluorescence quantum yield, $\Phi_f < 10^{-3}$. A decrease in solvent polarity causes almost a three-orders-of-magnitude increase in Φ_f and τ.

Results and Discussion

To explore the benefits of amphipathic derivatives of ANI, we introduce a primary amine to its imide nitrogen via an 1,2-ethylene linker, i.e., **ANI-NH$_2$** (Scheme 1).

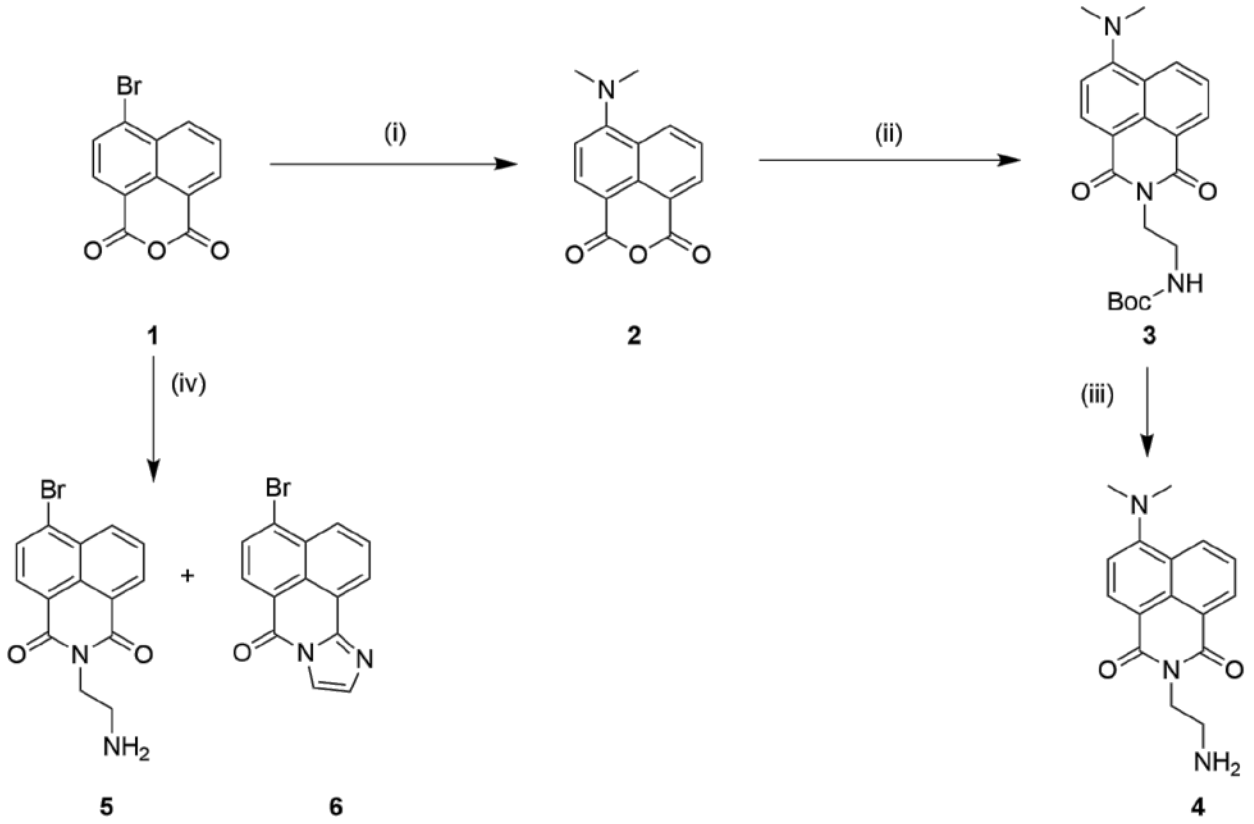

Scheme 1. The two synthetic routes of making ANI-NH$_2$ are depicted however only one was used. (i) 3-dimethylaminopropenitrile, reflux, 2hr (86%) (ii) *N*-Boc-ethylenediamine, toluene, reflux, 2hr (74%) (iii) trifluoroacetic acid, DCM, r.t. 2hrs (70%) (iv) *N*-ethylenediamine, reflux.

Nucleophilic aromatic substitution allows facile preparation of the **2** in excellent yields. Normally ,acidic medium and elevated temperature catalyzes imide formation to create the naphthalimides. However, the acid and temperature sensitivity of the *t*-Boc protection group renders such optimal conditions unfeasible for the preparation of **3**. Conversely, direct synthesis of **ANI-NH$_2$** from **2**, using unprotected 1,2-ethylenediamine, leads to a stable side product **6**, via immination of one of

the carbonyls (Scheme 1). Therefore, we adopt conditions without an acid catalyst to produce **3**, the acidic hydrolysis of which leads to **ANI-NH2 (4)** in quantitative yields (Scheme 1).

The solubility of **ANI-NH2** in a broad variety of solvents, such as hexanes, alcohols and water, allows for facile examination of its solvatochromic properties. An increase in solvent polarity causes: (1) bathochromic shifts in the optical absorption and emission spectra of **ANI-NH2** (Figure 1), and (2) a decrease in its fluorescence quantum yield, ϕ_f, and excited-state lifetime, τ (Table 1).

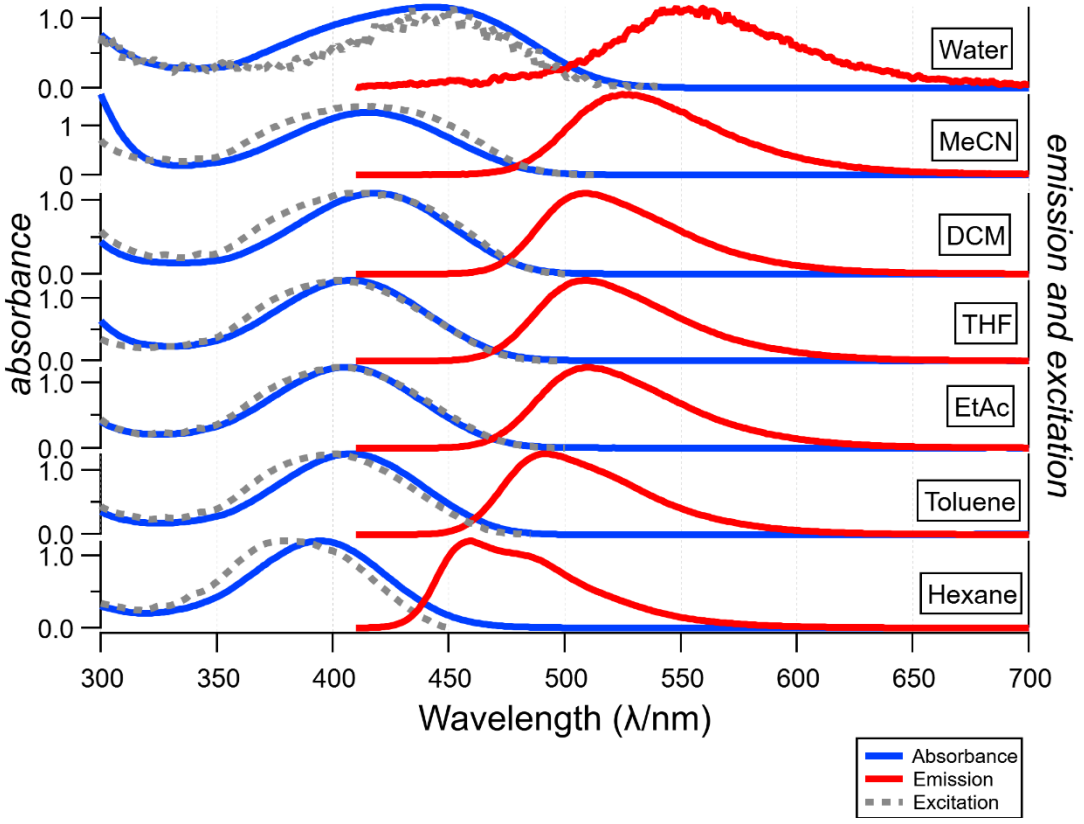

Figure 1. Optical spectra of ANI--NH_2 in various polarity solvents.

	Dielectric Constant ε	τ (ns)	k_f ($x10^8$ s^{-1})	k_{nr} ($x10^8$ s^{-1})
Water	78.54	0.0132	0.425	7.55
MeCN	36.64	0.953	0.208	10.3
DCM	8.93	10.2	0.449	0.528
THF	7.52	5.18	0.496	1.43
EtAc	6.25	3.19	0.543	2.59
Toluene	2.40	8.94	0.467	0.652
Hexanes	1.89	8.67	0.549	0.605

Table 1. Lifetime and radiative rates of ANI-NH_2 in various solvents

The former is consistent with the CT character of the lowest singlet excited state that polar media stabilize. The latter is consistent with a polarity-induced increase in the non-radiative decay rate constant, k_{nr}, while the radiative decay rate constant, k_f, remains practically the same (Table 1 / Figure 2). Polarity was measured using the Onsager function, the calculated values are tabulated (Table 2).

	Dielectric Constant ε	Refractive Index n	Born Solvation	Onsager Solvation
Water	78.54	1.333	0.550	0.639
MeCN	36.64	1.344	0.526	0.609
DCM	8.93	1.424	0.381	0.434
THF	7.52	1.407	0.372	0.418
EtAc	6.25	1.372	0.371	0.407
Toluene	2.40	1.496	0.0301	0.306
Hexanes	1.89	1.375	-1.74×10^{-4}	-1.64×10^{-4}

Table 2. The Onsager solvation values were calculated and used for various graphs. Onsager values were used to calculate the polarity using the function: $\Delta f_O(\varepsilon,n^2) = f_O(\varepsilon) - f_O(n^2)$, where $f_O(x) = 2(x-1)/(2x+1)$, where ε is the dielectric constant and n is the refractive index of the solvent.

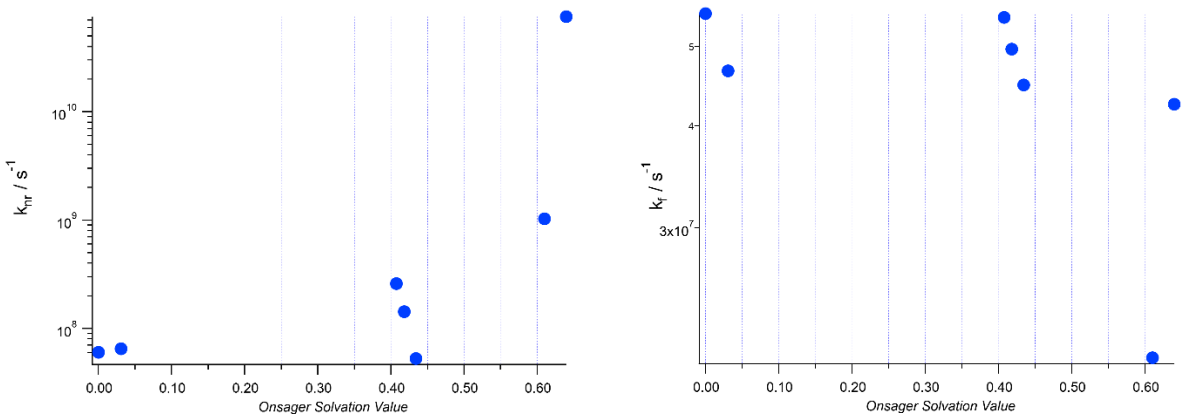

Figure 2. On the left is the correlation of nonradiative decay rates based on polarity and on the right are the radiative decay rates compared with the polarity of the solvent.

In the nonpolar hydrocarbon solvents, the emission spectra exhibit shoulders at their bathochromic sides, attributed to two overlapping bands (Figure 1). This shoulder formation is indicative of the presence of two emissive species of the dye in non-polar media. Ascribing the short-wavelength fluorescence band to emission from the Franck-Condon (FC) excited state and the long-wavelength one, responsible for the shoulder features, to emission from a twisted intramolecular charge-transfer (TICT) state, presents a plausible reason for the polarity-induced increase in k_{nr} (Table 1).

The relatively small values of k_f, ranging between 1×10^7 s^{-1} and 5×10^7 s^{-1}, are characteristic for small transition dipole moments between CT excited states with separated electrons and holes, and ground states with a reasonable π-conjugation between the electron donating and accepting moieties. The sizable increase in the Stokes' shift with the increase in solvent polarity (Figure 3) is consistent with different dipole moments of the ground and the excited state, and with the CT character of the emissive singlet excited state.

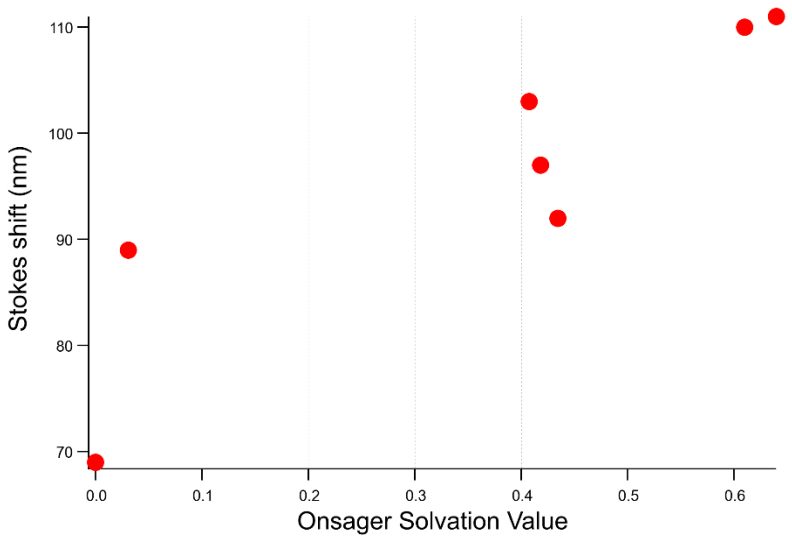

Figure 3. The trend between polarity and stokes shifts (the difference between the absorbance maxima and emission maxima).

While aromatic dialkyl amines with electron withdrawing groups, such as ANI derivatives, have a propensity for forming twisted intramolecular charge-transfer (TICT) excited states(Singha et al., 2015)(Haidekker & Theodorakis, 2010) the photophysical properties of **ANI-NH$_2$** do not show apparent correlations with the solvent viscosity (Figure 4). These finding suggests that the viscosity is not affecting the energy barrier of the locally excited (LE) state and the TICT state and emission any emission shifts are occurring due to the TICT state. The viscous solvents used were all polar protic, when comparing the emission shifts as a measure of polarity rather than viscosity it further confirms that the energy barrier between the LE state and the TICT is not affected by the viscosity. The dimethylamine nitrogen to the carbon on the aromatic is the position that twists to for the TICT state. The substituents on the amine are two methyl groups which are relatively small and the rate at which it rotates is relatively fast and should not be affected significantly by the viscous solvent.

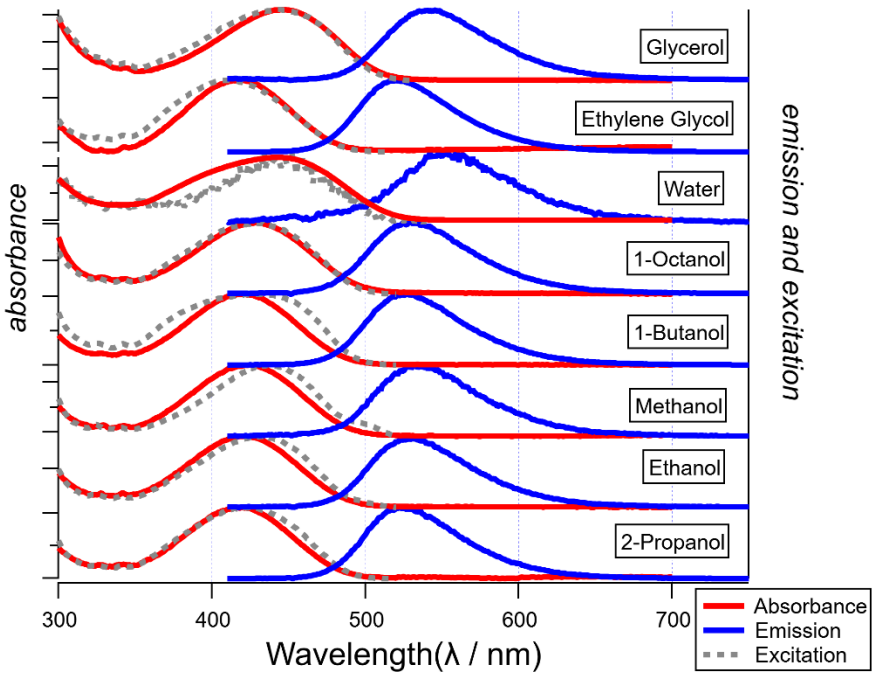

Figure 4. The absorbance, emission, and excitation of ANI-NH_2 in various viscous solvents is shown in decreasing order of viscosity.

While the evidence show that the medium polarity is the principle reason for the observed trends in the optical properties of **ANI-NH_2**, hydrogen bonding with the solvent can strongly affect the photophysics of carbonyl-containing chromophores(Singha et al., 2015). The solvent proticity, however, has no detectable effects on ϕ_f and τ of **ANI-NH_2**. The trends for alcohols with different polarities overlap well with those for aprotic solvents (Figure 5).

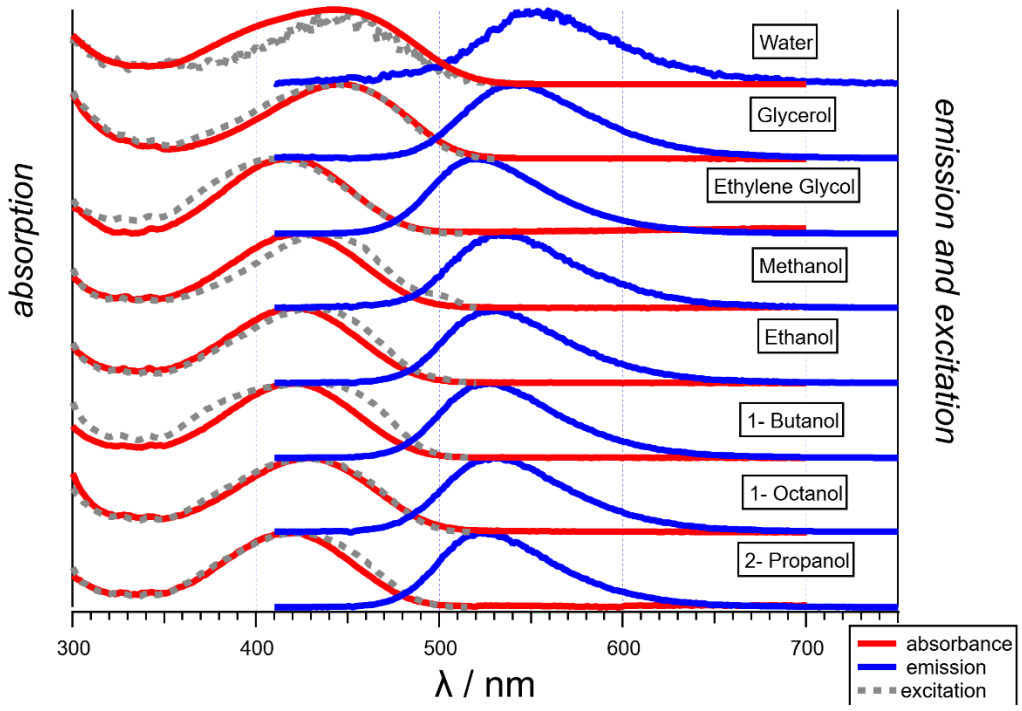

Figure 5. The alcohols used to check for a viscosity trend have been arranged in decreasing polarity and their optical properties can be compared.

Transient-absorption (TA) spectroscopy elucidates further the solvent dependence of the excited-state dynamics of **ANI-NH$_2$**. A sharp TA band at 450 nm, stimulated emission (SE) at 500 nm, and a broad TA band at 800 nm are characteristic for the singlet excited state of ANI--NH$_2$ in toluene (Figure 6).

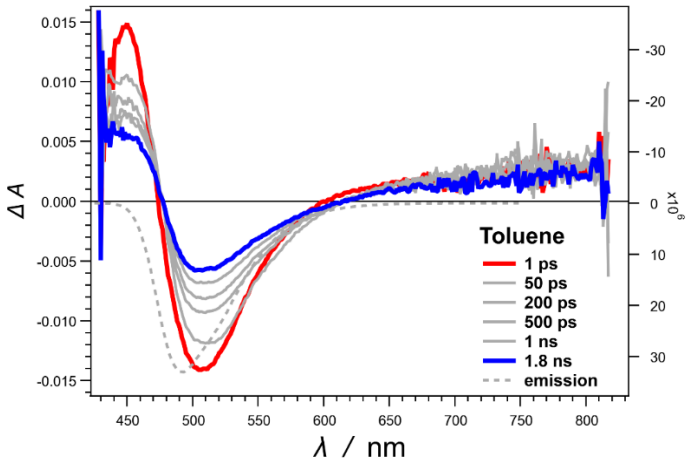

Figure 6. The representative kinetics of ANI-NH_2 in toluene are shown with significant bands at 450 nm, 500 nm, and 800 nm.

Global-fit analysis reveals a picosecond decay of the 450-nm TA band and the SE signal with a rate constant, *k*, of about 1.4×10^{10} s^{-1}, followed by a nanosecond decay ($k = 1.1\times10^{8}$ s^{-1}) of the two TA bands and the SE signal (Figure 6).

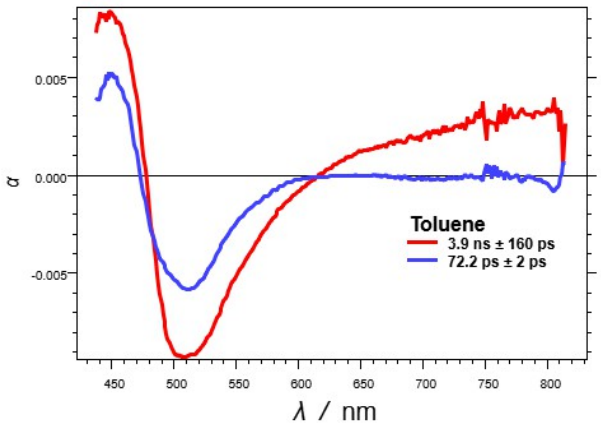

Figure 7. Global fit analysis of ANI-NH_2 in toluene and its decay rates

An increase in solvent polarity accelerates the deactivation kinetics of the ANI-NH_2 emissive excited states. For water, **ANI-NH_2** shows TA peaking at 520 nm that overlaps with the SE band

at 560 nm and the ground-state bleach at 470 nm, in addition to a broad TA band around 750 nm (Figure 8). A picosecond decreases in SE ($k = 3.4\times10^{11}$ s^{-1}) accompanies a arise of the 750-nm TA band (Figure 8). A slower decay of the two TA bands with $k = 7.6\times10^{10}$ s^{-1}, which follows, along with a bleach recovery and a further SE decrease, brings the ΔA signals to the baseline in about 50 ps (Figure 8).

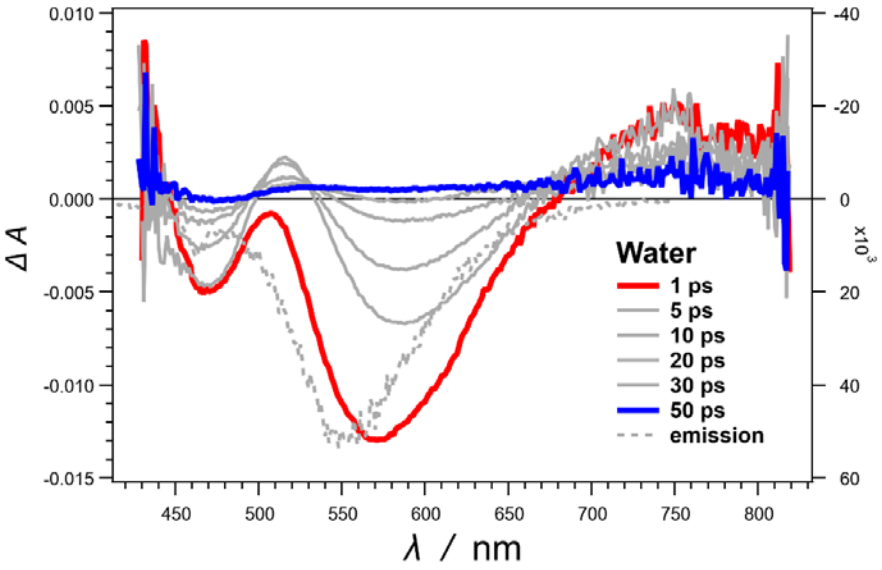

Figure 8. The representative kinetics of ANI-NH_2 in water are shown with significant bands at 470 nm, 520nm, 560 nm, and 750 nm.

The TA dynamics is consistent with the formation of two emissive excited state: a short-lived CT state, and a long-lived TICT state. The single photon counting experiments of ANI-NH_2 in polar solvents are composed of two components, a fast and a slow one indicating two species (Figure 9). The fast corresponding to the CT state and the slow to the TICT state further confirming the TA data.

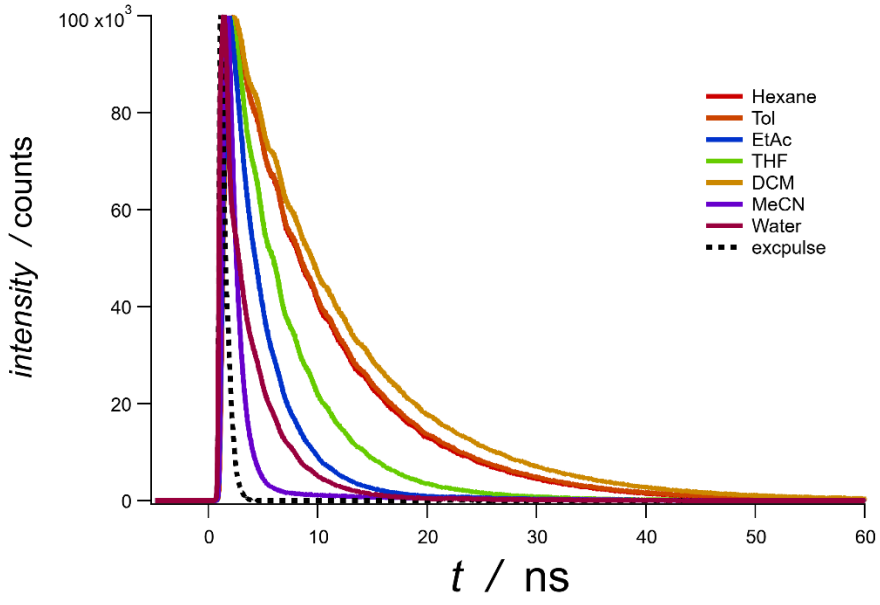

Figure 9. Time resolved single photon counting experiments are shown for ANI-NH_2 in various polarity solvents.

Protic solvents with pronounced acidity, such as fluorinated alcohols, can affect the photophysics of aromatic amines.(Krystkowiak et al., 2014) Hydrogen-bonding or protonating of aromatic amines decreases their electron-donating propensity in push-pull conjugates, such as **ANI-NH_2**, and strongly affects their excited states with a CT character. Subjecting **ANI-NH_2** to acidic media leads to a decrease in the molar absorptivity and hypsochromic shift of the visible band (Figure 10) that accompanies an increase in ϕ_f.

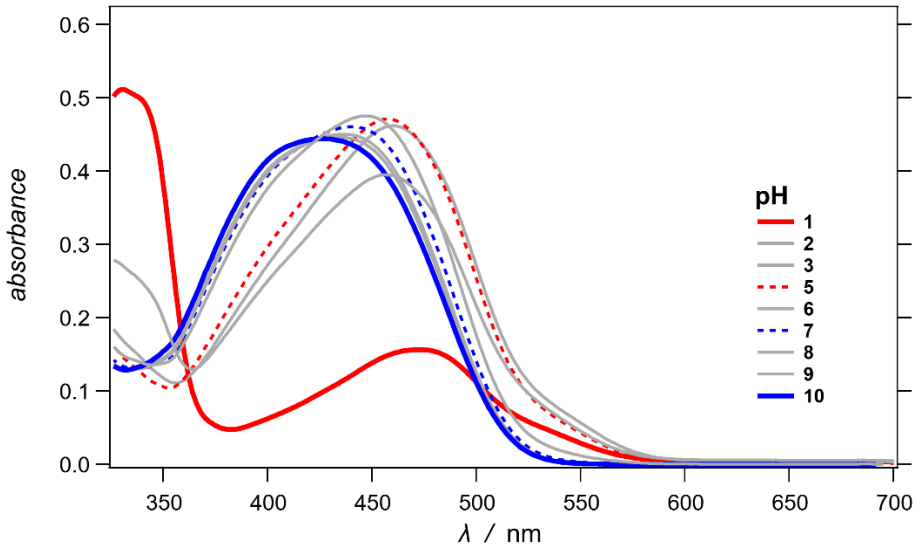

Figure 10. pH dependence measurements were made using 40μM ANI in commercially available buffers.

We ascribe these drastic spectral changes to the protonation of the aromatic tertiary amine of **ANI-NH2**, for which the pH dependence yields a pK_a value of 2.2 (Figure 11), which is expected for pK_a of anilinium ions derivatized with electron-withdrawing groups.

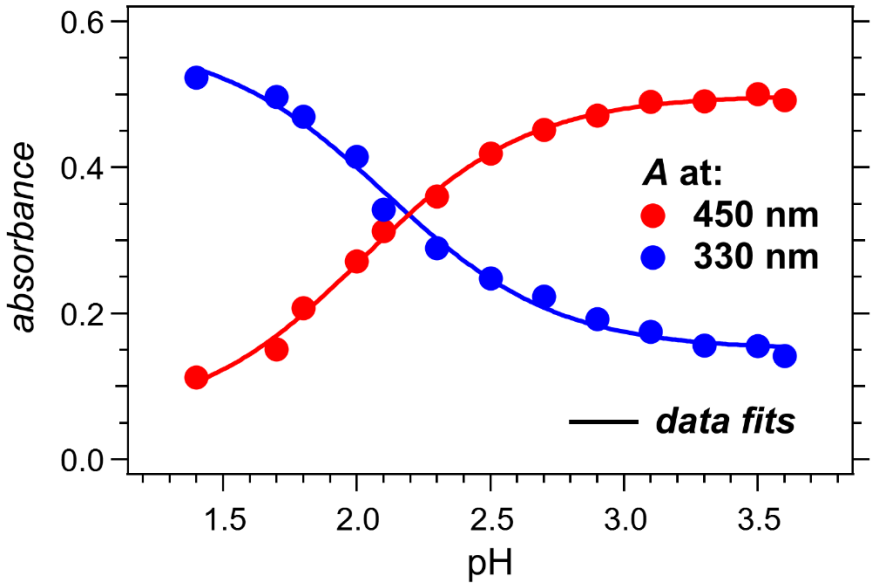

Figure 11. Using the absorption at 450 nm and 330 nm at different pH we can calculate the pKa as the intersection of the two fits. These wavelengths were used as they were the peak of the two absorption bands.

These findings show that protonating the dimethylamine affects the CT excited state of ANI-NH_2 by: (1) elevating its energy level, (2) decreasing the transition dipole moment to it, and (3) suppressing the its non-radiative deactivation.

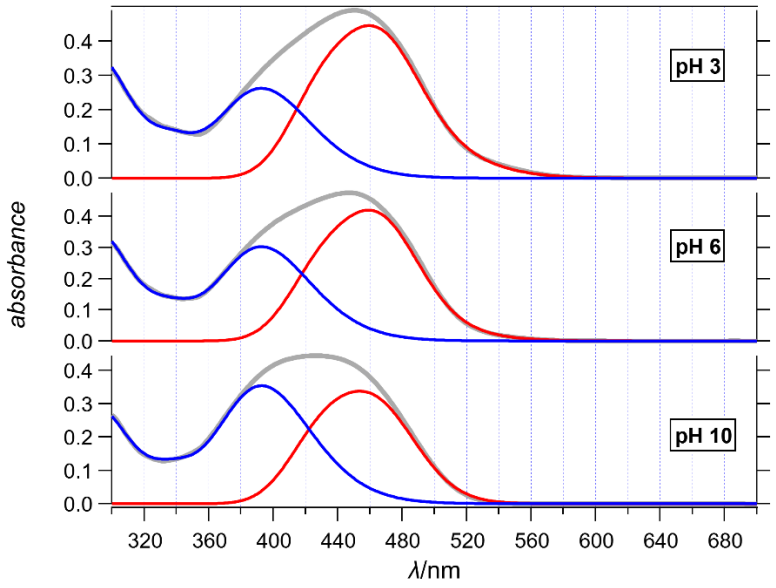

Figure 12. Absorbance spectra of ANI-NH_2 at pH 3, 6, and 10 are deconvoluted (red and blue) to show the two transitions that make up spectral shifts.

Except under extreme conditions, such as acidophile media, lysosome microenvironment and stomach interior, the pK_a of the protonated tertiary amine of **ANI-NH_2** has no real biological relevance. Encompassing physiological conditions, however, varying the pH of the aqueous medium between 3 and 10 reveals a subtle change in the spectra of **ANI-NH_2** (Figure 12). Spectral

deconvolution shows that changes of the relative contributions from two overlapping transitions can account for the bathochromic shift and the slight decrease in molar absorptivity as the pH increases from 3 to 10 (Figure 12).

Experimental

Aminonaphthalimide is defined as a 2-(2-aminoethyl)-6-(dimethylamino) naphthlimide. Its unique characteristics include the dimethylamine and the free amine attached to the alkyl chain. These substituents contribute to ANI--NH_2's unique photophysical properties. Below are the methods used to synthesize and study its photophysical properties.

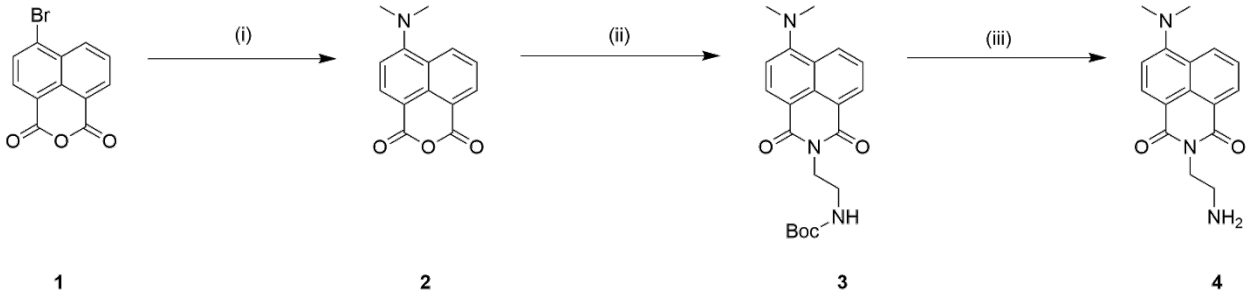

Scheme S1. (i) 3-dimethylaminopropenitrile, reflux, 2hr (86%) (ii) *N*-Boc-ethylenediamine, toluene, reflux, 2hr (74%) (iii) trifluoroacetic acid, DCM, r.t. 2hrs (70%)

6-(dimethylamino)-1H,3H-benzo[de]isochromene-1,3-dione (2) (Scheme S1). 4-Bromo-1'8-Naphthalic Anhydride (**1) (1 eq, 1.804 mmol, 500 mg)** and 3-dimethylaminopropenitrile (10 eq, 18.04 mmol, 2 mL) were placed in a round bottom and refluxed for 2 hours. The reaction was allowed cooled to room temperature, crystals formed (brown-orange color). The crystals were washed with milli Q water and subsequently dried under vacuum. Reaction yields 747.11 mg, 85.8% yield. HRMS (ESI) m/z Calculated Mass: 241.2460 Found Mass $(M+H)^+$ 242.0813 ^1H NMR (400 MHz, $CDCl_3$) δ 8.56 (dd, J = 7.3, 1.2 Hz, 1H), 8.52 – 8.42 (m, 2H), 7.68 (dd, J = 8.5, 7.3 Hz, 1H), 7.10 (d, J = 8.3 Hz, 1H), 3.18 (s, 6H).

*tert-butyl (2-(6-(dimethylamino)-1,3-dioxo-1H-benzo[de]isoquinolin-2(3H)-yl)ethyl)carbamate (**3**) (Scheme S1)* The solution of **2 (1 eq. 3.09 mmol, 747.1 mg in toluene (5 mL))** was added to the solution of *N*-Boc-ethylenediamine (1.5 eq, 4.64 mmol, 510 μL in toluene (5 mL)) and refluxed for 2 hours. The reaction mixture was evaporated under reduced pressure and purified by flash column chromatography (1:9 Ethyl Acetate: Dichloromethane). 880 mg, 74.2% yield. HRMS (ESI) m/z Calculated Mass: 383.4480 Found Mass $(M+Na)^+$ 406.1745 ^{1}H NMR (600 MHz, $CDCl_3$) δ 8.63 – 8.59 (m, 1H), 8.51 (d, *J* = 8.2 Hz, 1H), 8.48 (dd, *J* = 8.5, 1.2 Hz, 1H), 7.69 (dd, *J* = 8.5, 7.3 Hz, 1H), 7.15 (d, *J* = 8.2 Hz, 1H), 4.39 (t, *J* = 5.8 Hz, 2H), 3.55 (q, *J* = 5.7 Hz, 2H), 3.14 (s, 6H), 2.20 (s, 1H), 1.34 (s, 9H).

*2-(2-aminoethyl)-6-(dimethylamino)-1H-benzo[de]isoquinoline-1,3(2H)-dione (**4**)(Scheme S1)*

3 (100 mg, 0.352 mmol) was dissolved in dichloromethane (5 mL) and subsequently trifluoracetic acid (5 mL) was added. The reaction was stirred for 2 hours, after it was cooled water was added and sodium carbonate was slowly added until a pH of 8 was obtained. The organic phase was extracted with more dichloromethane and washed with brine. Reaction mixture was dried with sodium sulfate and evaporated. 453 mg, 70% yield. HRMS (ESI) m/z Calculated Mass: 283.3310 Found Mass $(M+H)^+$ 284.1660 ^{1}H NMR (600 MHz, DMSO) δ 8.56 – 8.51 (m, 1H), 8.49 – 8.43 (m, 1H), 8.35 (d, *J* = 8.3 Hz, 1H), 7.85 (s, 2H), 7.80 – 7.74 (m, 1H), 7.23 (d, *J* = 8.3 Hz, 1H), 4.29 (t, *J* = 6.0 Hz, 2H), 3.14 (s, 2H), 3.10 (s, 6H).

UV-VIS Absorbance and Fluorescence Spectroscopy. The absorbance spectra were recorded using a Varian Cary 50 UV/Visible spectrophotometer. Fluorescence measurements were conducted with a Horiba Jobin Yvon Fluorolog-3-22 spectrofluorometer. We compare the optical properties of ANI-NH_2 in different polarity solvents.

Transient Absorption Spectroscopy. Measurements were done using the Helios Femtosecond Transient Absorption spectrometer.

Conclusion

Fluorescent dyes are essential for labelling distinct cell subunits and finding readily available dyes that have this capacity is crucial to understanding events occurring at subcellular levels. Naphthalimides are known for their specificity and relatively simple synthesis. ANI-NH_2 was synthesized and its spectral properties were used to characterize it. ANI-NH_2 demonstrated solvatochromatic properties which can be attributed to the charge transfer occurring within the molecule. These charge transfer characteristics come from the amine moieties at each end. Further studies also show that ANI-NH_2 forms a TICT state more readily in polar solvents, due to dipole relaxations. As ANI-NH_2 is excited from the ground state to the Frank Cordon state where the charge transfer can occur, if the TICT state is not formed it emits from the locally excited state and has longer lifetimes and higher quantum yields. This exemplifies the importance of ANI-NH_2 as a dye seeing its photophysical properties allow for studying microenvironments of subcellular systems.

Future Work

In lieu of the pandemic, the project was delayed from its bigger picture purpose. ANI-NH_2 is meant to be used as a dye in single molecular mechanic studies using enzymes and inhibitors. Enzyme-inhibitor interactions are essential for understanding root causes of certain diseases. The

rates of interaction and the strength of bonding affect a variety of diseases. Therefore,

understanding of the enzyme-inhibitor interactions is essential for advancing basic science and

for developing new medical paradigms. Using magnetic forces, we can study protein mechanics at a single-molecule level to determine the kinetic characteristics of the of interactions between enzymes and inhibitors. Single-molecule studies are indispensable for discovering rare events that have immense biomedical importance but are statistically insignificant to be detectable with conventional bulk measurements. The challenge is to systematically work with weak forces (1 – 20 pN) that are applied through micrometer size transducers, i.e., magnetic beads that also serve as probes for following molecular motion; and apply these forces specifically to a single enzyme-inhibitor complex without involving non-specific interactions. Employing entropic repulsion allows for suppression non-specific interactions. Another challenge is to image the superparamagnetic beads with an inverted microscope that has magnetic assembly above the field of view. ANI-NH_2 is meant to be used as a fluorescent tag on the bead surface under the biocompatible coatings. ANI-NH_2 is best suited for these experiments because it is water soluble and sustains the reaction conditions of reductive amination that we use. ANI-NH_2 would provide a means for improving the sensitivity of the imaging tracking that is used for following single-molecule events. These studies will provide the first experimental means for detection of transition states and for discerning directionality of interactions.

Acknowledgements

This work was supported by Award Number T34GM062756 from the National Institutes of Health and the University of California Riverside Office of Undergraduate Education Mini Grant.

References

Anderson, G. F., & Chu, E. (2007). Expanding priorities - Confronting chronic disease in countries with low income. *New England Journal of Medicine*. https://doi.org/10.1056/NEJMp068182

Caldwell, D. E., Korber, D. R., & Lawrence, J. R. (1992). Imaging of bacterial cells by fluorescence exclusion using scanning confocal laser microscopy. *Journal of Microbiological Methods*. https://doi.org/10.1016/0167-7012(92)90045-6

Domcke, W., & Yarkony, D. R. (2012). Role of Conical Intersections in Molecular Spectroscopy and Photoinduced Chemical Dynamics. *Annual Review of Physical Chemistry*. https://doi.org/10.1146/annurev-physchem-032210-103522

Eilers, Y., Ta, H., Gwosch, K. C., Balzarotti, F., & Hell, S. W. (2018). MINFLUX monitors rapid molecular jumps with superior spatiotemporal resolution. *Proceedings of the National Academy of Sciences of the United States of America*. https://doi.org/10.1073/pnas.1801672115

Ettinger, A., & Wittmann, T. (2014). Fluorescence live cell imaging. In *Methods in Cell Biology*. https://doi.org/10.1016/B978-0-12-420138-5.00005-7

Gonçalves, M. S. (2010). Advanced Fluorescence Reporters in Chemistry and Biology I. Fundamentals and Molecular Design. In *Advanced Fluorescence Reporters in Chemistry and Biology I SE - 2*. https://doi.org/10.1007/978-3-642-04702-2_2

Haidekker, M. A., & Theodorakis, E. A. (2010). Environment-sensitive behavior of fluorescent molecular rotors. In *Journal of Biological Engineering*. https://doi.org/10.1186/1754-1611-4-11

Heitele, H., Finckh, P., Weeren, S., Pöllinger, F., & Michel-Beyerle, M. E. (1989). Solvent polarity effects on intramolecular electron transfer. 1. Energetic aspects. *Journal of Physical*

Chemistry. https://doi.org/10.1021/j100350a030

Krystkowiak, E., Dobek, K., & Maciejewski, A. (2014). Deactivation of 6-aminocoumarin intramolecular charge transfer excited state through hydrogen bonding. *International Journal of Molecular Sciences*. https://doi.org/10.3390/ijms150916628

Li, L., Guo, W., Yan, Y., Lee, S., & Wang, T. (2013). Label-free super-resolution imaging of adenoviruses by submerged microsphere optical nanoscopy. *Light: Science and Applications*. https://doi.org/10.1038/lsa.2013.60

Liu, T. L., Upadhyayula, S., Milkie, D. E., Singh, V., Wang, K., Swinburne, I. A., Mosaliganti, K. R., Collins, Z. M., Hiscock, T. W., Shea, J., Kohrman, A. Q., Medwig, T. N., Dambournet, D., Forster, R., Cunniff, B., Ruan, Y., Yashiro, H., Scholpp, S., Meyerowitz, E. M., … Betzig, E. (2018). Observing the cell in its native state: Imaging subcellular dynamics in multicellular organisms. *Science*. https://doi.org/10.1126/science.aaq1392

Majumdar, D. K., & Basu, S. (1960). Charge transfer and fluorescence quenching. *The Journal of Chemical Physics*. https://doi.org/10.1063/1.1731356

Rust, M. J., Bates, M., & Zhuang, X. (2006). Sub-diffraction-limit imaging by stochastic optical reconstruction microscopy (STORM). *Nature Methods*. https://doi.org/10.1038/nmeth929

Sahl, S. J., & Moerner, W. E. (2013). Super-resolution fluorescence imaging with single molecules. In *Current Opinion in Structural Biology*. https://doi.org/10.1016/j.sbi.2013.07.010

Singha, S., Kim, D., Roy, B., Sambasivan, S., Moon, H., Rao, A. S., Kim, J. Y., Joo, T., Park, J. W., Rhee, Y. M., Wang, T., Kim, K. H., Shin, Y. H., Jung, J., & Ahn, K. H. (2015). A structural remedy toward bright dipolar fluorophores in aqueous media. *Chemical Science*. https://doi.org/10.1039/c5sc01076d

Smith, K. M., Machalaba, C. C., Seifman, R., Feferholtz, Y., & Karesh, W. B. (2019). Infectious disease and economics: The case for considering multi-sectoral impacts. In *One Health*. https://doi.org/10.1016/j.onehlt.2018.100080

Thomas, M. S., Nuñez, V., Upadhyayula, S., Zielins, E. R., Bao, D., Vasquez, J. M., Bahmani, B., & Vullev, V. I. (2010). Kinetics of bacterial fluorescence staining with 3,3′-diethylthiacyanine. *Langmuir*. https://doi.org/10.1021/la1013279

Upadhyayula, S., Nuñez, V., Espinoza, E. M., Larsen, J. M., Bao, D., Shi, D., Mac, J. T., Anvari, B., & Vullev, V. I. (2015). Correction: Photoinduced dynamics of a cyanine dye: Parallel pathways of non-radiative deactivation involving multiple excited-state twisted transients. In *Chemical Science*. https://doi.org/10.1039/c5sc90020d

Upadhyayula, S., Quinata, T., Bishop, S., Gupta, S., Johnson, N. R., Bahmani, B., Bozhilov, K., Stubbs, J., Jreij, P., Nallagatla, P., & Vullev, V. I. (2012). Coatings of polyethylene glycol for suppressing adhesion between solid microspheres and flat surfaces. *Langmuir*. https://doi.org/10.1021/la300545v

Wahadoszamen, M., Margalit, I., Ara, A. M., Van Grondelle, R., & Noy, D. (2014). The role of charge-transfer states in energy transfer and dissipation within natural and artificial bacteriochlorophyll proteins. *Nature Communications*. https://doi.org/10.1038/ncomms6287

Xia, B., Upadhyayula, S., Nuñez, V., Landsman, P., Lam, S., Malik, H., Gupta, S., Sarshar, M., Hu, J., Anvari, B., Jones, G., & Vullev, V. I. (2011). Amyloid histology stain for rapid bacterial endospore imaging. *Journal of Clinical Microbiology*. https://doi.org/10.1128/JCM.02285-10

Zhao, J., Chen, J., Ma, S., Liu, Q., Huang, L., Chen, X., Lou, K., & Wang, W. (2018). Recent developments in multimodality fluorescence imaging probes. In *Acta Pharmaceutica Sinica*

B. https://doi.org/10.1016/j.apsb.2018.03.010